9^{th} *LISA Symposium, Paris*
ASP Conference Series, Vol. 467
G. Auger, P. Binétruy and E. Plagnol, eds.

LIGO/Virgo/GEO/KAGRA Science

Riccardo Sturani

Università degli studi di Urbino 'Carlo Bo' I-61029

INFN, Sezione di Firenze, I-50019 Sesto Fiorentino, Italy

Abstract. A network of ground based detectors of gravitational waves will start operating in their advanced phase in about three years from now. After briefly reviewing the scientific results which have been obtained in past observational activities by LIGO and Virgo, the foreseeable consequences of a detection of gravitational wave for astrophysics, cosmology and fundamental physics are presented.

1. Introduction

The improvement of a network of earth-based, kilometer-sized interferometers is currently under development. The two Laser Interferometer Gravitational-Wave Observatory (LIGO) placed, respectively, at Hanford (Washington, USA) and Livingstone (Louisiana, USA) are undergoing an upgrade to their advanced stage after taking data for several years. Similarly the Virgo interferometer, placed near Pisa (Italy), is currently being upgraded after taking part in joint science run activities together with the LIGO detectors. The data taking activity of the LIGO and Virgo detectors is scheduled to resume around the end of the year 2014, which should mark the start of the advanced detector era, even if few years are expected to elapse before the advanced detector planned sensitivities, as displayed in fig.1a, could be reached. Another detector belonging to the network is the German-British gravitational wave observatory (GEO), which is currently taking data, but given the reduced size of its arms, 600m as compared to the 4(3) km of the LIGOs (Virgo), is not expected to make a detection on its own before the onset of the advanced detector era, when the full network will be operating.

The gravitational detector network is planned to be joined by the KAGRA detector, a 3 km arm cryogenic interferometer located in the Kamioka mine (Japan) around the end of this decade. At the beginning of the next decade another interferometer, placed in India, is expected to join in.

The sensitivities achieved by the detectors in the past are displayed in fig.1b and their scientific results, i.e. upper limits so far obtained, summarised in sec. 2. In sec. 3 an overview is given of the main expectations for the advanced detector era in terms of scientific results in astrophysics, fundamental physics and cosmology.

2. The earth-based GW detectors and the past searches

During past years the LIGO and Virgo detectors have performed several joint observation runs, which have not detected any gravitational wave (GW) signal, but which have

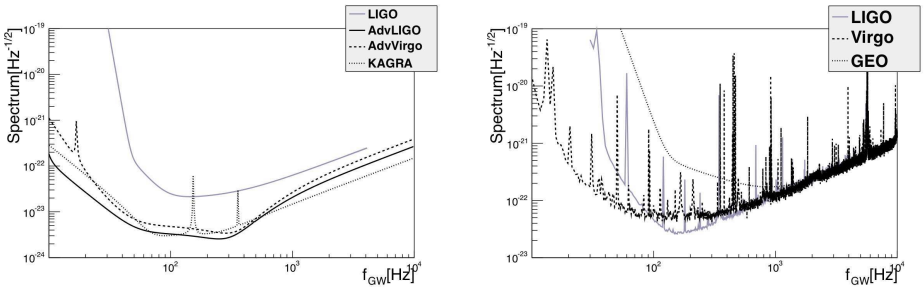

Figure 1. Expected sensitivities for Advanced LIGO/Virgo and KAGRA, compared with the design sensitivity of initial LIGO (left) and actual experimental sensitivities obtained by the LIGO and Virgo detectors during their initial and "plus" runs, ended respectively in October 2010 and September 2011, with a typical present GEO sensitivity (right).

set non-trivial upper limits on the amount of gravitational radiation emitted by astrophysical/cosmological sources and represented a valuable testing ground to set up and consolidate data analysis methods and search strategies.

A generic kind of GW signal is represented by a short transient ($\lesssim 1$ sec) or *burst*, which can be generated by a variety of astrophysical sources: merging compact binary systems consisting of black holes and/or neutron stars, core-collapse supernovae, neutron star collapse to black holes, star-quakes associated with magnetar flares, pulsar glitches, cosmic string cusps, to mention only some of the known GW generation mechanisms.

The result of a search for generic burst signals in the band 64Hz-5kHz has been reported in Abadie et al. (2012a), setting upper limits on events occurring at different frequencies, see fig.2a, and on the amount of energy in GWs that can be emitted by signals centred at different frequencies. In fig.2b different analytical models for the burst shape have been considered, with minor impact on the numerical result. For reference, the typical metric perturbation h generated by an event that released $E_{\rm GW} \sim 10^{-7} M_\odot$ at a distance $D \sim 10$ kpc from the earth, centred at $f_0 \sim 1$ kHz and lasting for $T \sim 1$ msec is

$$h \sim 5 \cdot 10^{-21} \left(\frac{E_{\rm GW}}{10^{-7}\, M_\odot}\right)^{1/2} \left(\frac{1\,\text{msec}}{T}\right)^{1/2} \left(\frac{1\,\text{kHz}}{f_0}\right)\left(\frac{10\,\text{kpc}}{D}\right). \quad (1)$$

With the perspective of a tenfold increase in amplitude sensitivity, sources one hundred times less energetic could be probed, reaching interesting $E_{\rm GW}$ value, at least for galactic sources ($D \lesssim 30$ kpc).

Also targeted searches has been considered, as a coincidence between electromagnetic or neutrino triggers on one side and GW triggers on the other, may increase the confidence of a marginal GW detection. A search have been performed in Abadie et al. (2011b) to check for coincidences of GW triggers from the LIGO/Virgo/GEO network with 1217 soft Gamma Ray Bursts (GRBs) from 5 Soft Gamma Repeaters and 1 Anomalous X-Ray pulsar associated with magnetars at a distance between 1 and 15 kpc from the earth (with a 4 sec window), with the result that no associated GW event has been detected. The electromagnetic luminosity $\mathcal{L}$ of the two brightest magnetars

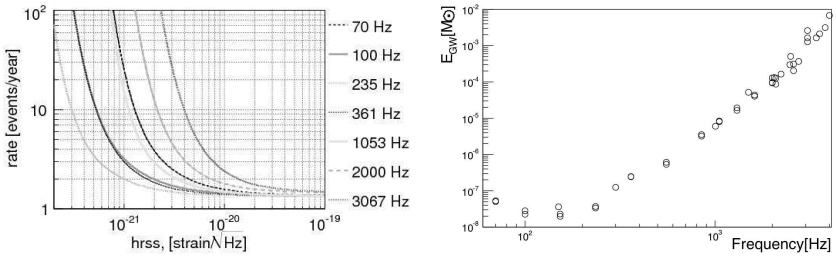

Figure 2. Main results of the burst search using 2009 and 2010 LIGO and Virgo data: upper limits on burst rate (a) and energy released from sources at 10 kpc (b) for different signal central frequencies. From Abadie et al. (2012a).

is $\mathcal{L} \sim 4 \cdot 10^{33}$erg/s, with a total radiated energy of $\sim 10^{54}$ erg. The upper limit on the amount of GW released in each burst event varies considerably with the assumed GW shape model, ranging from 10^{44} to few 10^{51} erg, starting to approach the range of electromagnetic energies radiated in giant flares.

A search in coincidence with high energy neutrino events ($\gtrsim 100$ GeV) as detected by the ANTARES experiment has been performed and described in Adrian-Martinez et al. (2012). The search has been performed over 158 neutrino events recorded in the period February-September 2007, with a window of ±496 sec, with the result of placing an upper bound on the rate $\rho_{\mathrm{GW-HEN}}$ of coincident GW-High Energy Neutrino events of

$$\rho_{\mathrm{GW-HEN}} \lesssim 10^{-3}\mathrm{Mpc}^{-3}\mathrm{yr}^{-1}\left(\frac{E_{\mathrm{GW}}}{10^{-2}M_{\odot}}\right)^{-3/2} . \tag{2}$$

For comparison, the supernova rate (in the continuum limit) ρ_{SN} up to a distance D is, see Ando et al. (2005),

$$\rho_{SN} \simeq 5 \cdot 10^{-4}\mathrm{Mpc}^{-3}\mathrm{yr}^{-1} \tag{3}$$

showing that, once the design sensitivity will be reached by the advanced detectors, either a detection will be made, or the upper bound in eq. (2) can be turned into an astrophysically interesting one.

Another search for coincidences between electromagnetic and GW events have been considered in Briggs et al. (2012), where data chunks corresponding to time window (−600 to +60sec) overlapping with 150 GRBs have been analysed in search for GW burst events, and 24 GRBs in search for GW signals from inspiralling binaries (in which at least one of the two binary constituent was assumed to be a neutron star).

In the search for signals from inspiralling/coalescing binaries the detector output is processed via standard matched-filtering methods, where the experimental data are correlated with *template* waveforms. These techniques allow to dig the signal out of the detector output even if buried well below the noise floor, however the template has to match well enough the shape of the signal in the data, in contrast to burst searches which look for noise excesses of unknown shape. In figs. 3 the upper bounds obtained by these analyses are summarised. In fig.3a the cumulative distribution of the observed distances of the GRB is plotted together with the lower bound for the distances obtained via a burst search. In order to convert the bound of the signal amplitude into a bound on distance, a total radiated energy $10^{-4}M_{\odot} < E_{\mathrm{GW}} < 10^{-2}M_{\odot}$ has been assumed. Such

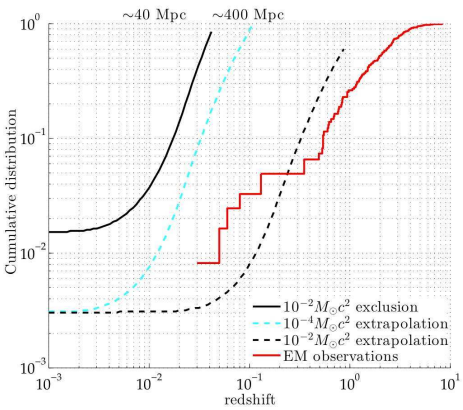

Figure 3a. Distance lower limit assuming an emitted $E_{\rm GW} = 10^{-2}M_\odot$ (solid black) and $E_{\rm GW} = 10^{-4}M_\odot$ (broken cyan). Also shown is the extrapolation to the advanced detector design sensitivity curve for $E_{\rm GW} = 10^{-2}M_\odot$.

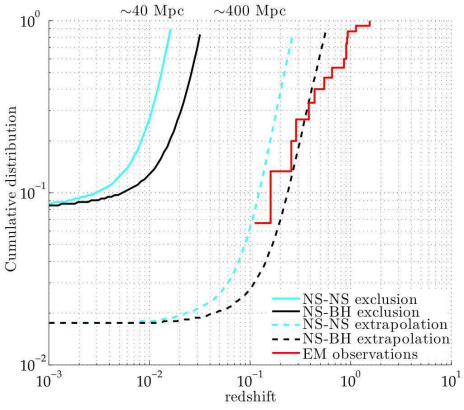

Figure 3b. Distance lower limit assuming signals from black hole/neutron star and double neutron star cases for actual sensitivity (solid lines) and the extrapolation for the advanced detector design sensitivity (dashed lines).

Figure 3. Result from GRB-triggered GW searches: fractional cumulative distance distribution of observed GRBs (solid red) versus fractional cumulative distance lower limit distribution from a burst search (a) and a matched-filtering one (b). From Briggs et al. (2012).

an energy interval represents a reasonable range for the energy emitted in GWs by coalescing binary systems involving at least one neutron star, see e.g. Maggiore (2008), as these systems are considered as serious candidate progenitors of short gamma ray bursts, see Piro (2005). Extrapolations are also shown in fig.3a for the advanced detector design sensitivity (broken lines). In fig.3b again the cumulative distance distribution lower bound is displayed, with the analysis performed in term of matched filtering with inspiral waveforms describing black hole/neutron star or double neutron star systems (masses $\sim 1.4\,M_\odot$ have been assumed for neutron stars and a mass distribution centred at $10\,M_\odot$ for black holes).
In both cases it appears that once advanced detector design sensitivity will be reached, with the consequent ten-fold increase in distance reach, either a detection will be made or upper bounds with non-trivial astrophysical scientific content will be set.

Untriggered searches for inspiralling binaries signals have also been performed, with the result summarised in fig.4, from Abadie et al. (2012b). The rate upper bounds are slightly different according to the type of binary system (double neutron star, mixed neutron star-black hole or double black hole, in order of increasing total mass), setting the rate of coalescences ρ_C to be $\rho_C < 10^{-4}\mathrm{Mpc}^{-3}\ \mathrm{yr}^{-1}$. However, with the sensitivity increase planned with the advanced detectors, such rate upper bounds will be moved into the range of astrophysical prediction (blue band in fig.4) as a ten-fold increase in sensitivity will allow to probe a thousand times larger volume. At design sensitivity for the advanced stage, the expected rate of detected coalescences of any type can range

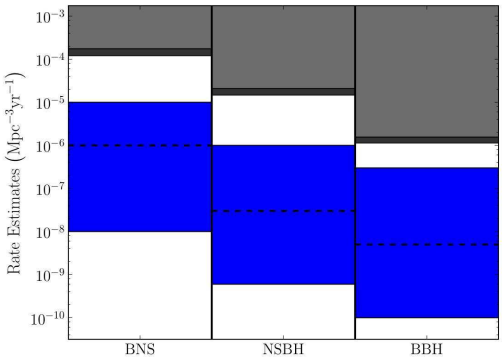

Figure 4. Upper bound on the rate of inspiralling binaries (light grey) improved by the last result in Abadie et al. (2012b) (dark grey), compared with astrophysical predictions (blue band). Dashed lines mark realistic values.

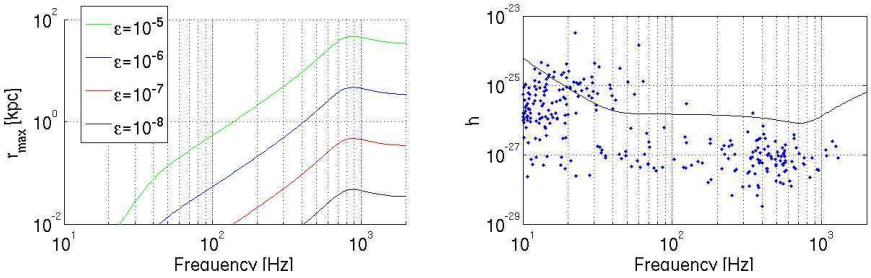

Figure 5. Detection prospects of periodic signals from pulsars by the advanced detectors at design sensitivity: maximum distance of detectability for a given ellipticity (a) and spin-down limit for known pulsars compared with GW sensitivity for 1 yr integration (b). Courtesy of C. Palomba.

from 0.4 to 400 per year, see Abadie et al. (2010), the relative horizon range for binary neutron star systems being 200 Mpc.

Another target of the experimental search are quasi-periodic signals, whose prototypical candidate sources are rotating, not rotationally symmetric neutron stars. Via the standard Einstein quadrupole formula, the gravitational luminosity of a compact object of mass M, of size R, with ellipticity ϵ, rotating with frequency f, is given by

$$L_{\mathrm{GW}} \simeq f^6 M^2 R^4 \epsilon^2 \,. \tag{4}$$

Since many neutron stars are electromagnetically visible as pulsars, the absence of a GW signal from known pulsars enables to set upper bounds on their ellipticities. For instance the Crab and Vela pulsar have been set respectively $\epsilon_C < 1.4 \cdot 10^{-4}$, see Abbott et al. (2010), and $\epsilon_V < 5 \cdot 10^{-4}$, see Abadie et al. (2011a). These limits beat indirect limits derived from energy conservation and the measured rate of deceleration of rotation, the so-called spin-down limits.

3. Science with future searches by advanced detectors

At present, evidence already exists that GWs are produced, via the rate of change of the orbital period of a handful of binary pulsars, see Weisberg & Taylor (1984). However, beside the intrinsic importance of making a direct detection of GWs, their repeated observation will open a new window onto the Universe, by giving birth to the field of GW astronomy.

A direct detection of GWs could shed light on a number of astrophysical and cosmological processes that include: probe the neutron star population independently of their electromagnetic emission, probe the black hole population in the 1 to few 100 $M_\odot$ mass range, provide a direct measure of the rate of binary coalescences, probe neutron star interior, i.e. test nuclear matter at very high density, verify the association between short GRBs and GWs, make tests of General Relativity (GR) in the strong-field regime, use coalescing binaries as standard sirens for cosmology. In the next subsection we will briefly outline the impact of GW science on these topics.

3.1. Astrophysics

The search for periodic signals from isolated neutron stars in the advanced detector era can probe values of ellipticities, see fig.2a, which are in the range of astrophysical expectations. Fig.2b shows the value of the spin-down limit for the *known* pulsars compared with the bound that advanced detectors will be able to set. Moreover, once GW detections from isolated neutron stars will be made, it is expected that neutron stars will be detected independently of their pulsating radio beam, which, contrary to the GW emission, is focused within a narrow angle around the axis of the magnetic field.

One of the most interesting target of GW search are coalescing binaries. The distance reach of the advanced detectors for such sources, see fig.6a, is increased with respect to the initial ones, not only because of an increased sensitivity, but also because the sensitive spectrum will extend to lower frequencies, allowing more massive systems to fall into the measurement band. The first part of the reach curve roughly grows as $M_c^{5/6}$, being $M_c \equiv (m_1 m_2)^{3/5} M^{2/5}$ ($m_{1,2}$ are the constituent masses of the binary systems and $M \equiv m_1 + m_2$). Beyond around 100 $M_\odot$ the inspiral phase falls off-band for the initial detector sensitivity curve, and the reach distance start decreasing as more and more power exits the visible band: for higher masses only the final merger and ring-down stages of the coalescence are visible. As shown in fig.6b, the signal from more massive binary systems is stronger but extends to smaller frequencies, so a sensitivity increase at the lowest edge of the spectrum is crucial for detecting more massive systems. The initial sensitivity detectors allowed to put an upper bound on the rate ρ_{25-100} of coalescences made by systems with mass range $25 < M/M_\odot < 100$ given by $\rho_{25-100} < 2$ Mpc^{-3} Myr^{-1}, see Abadie et al. (2011c), whereas theoretical predictions roughly range between 10^{-4} and few 10^{-1} Mpc^{-3} Myr^{-1} for black hole pairs, see Abadie et al. (2010), Signals from coalescing binaries with $M > 100$ have been also searched for in Abadie et al. (a), obtaining an upper limit on the rate of $\rho_{>100} \lesssim 1$ Mpc^{-3} Myr^{-1}.

Moreover, work is ongoing to ensure an electromagnetic follow-up by radio, optical and X bands with a short ($\sim 30\,min$) latency, see Abadie et al. (b) and Evans et al. (2012) for preliminary results of performing an electromagnetic search as a follow-up of a GW trigger. A good reconstruction of the sky position (within few square degrees) is however crucial for an electromagnetic follow-up observation. On the other hand sky

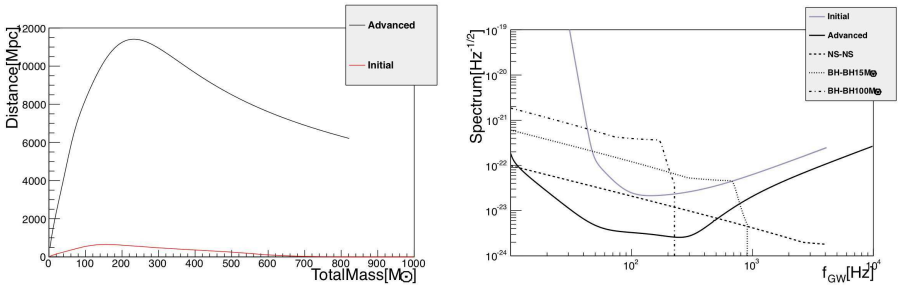

Figure 6. Distance reach versus total system mass for binary coalescence (a) and typical spectrum of non-precessing binary coalescing systems with different masses compared with strain sensitivity (b).

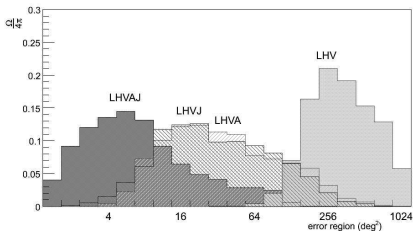

Figure 7a. Distribution of sky fraction of reconstructed source position vs. error region size for a burst analysis from Klimenko et al. (2011)

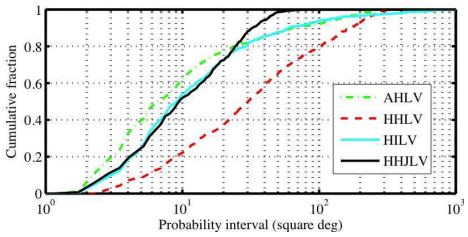

Figure 7b. Cumulative distribution of sky fraction reconstruction vs. error region size for inspiral signal injections. From Veitch et al. (2012)

Figure 7. Sky position reconstruction precision for different networks. H stands for LIGO Hanford, L=LIGO Livingstone, V=Virgo, J=KAGRA, I=LIGO India, A stands for a hypothetical LIGO in Western Australia.

position reconstruction of GW triggers heavily depends on the number of the detectors involved in the detection, as it mostly relies on time delay among detectors. Figs. 7 show distributions quantifying the fraction of the sky having a given sky position uncertainty, for different detector networks. They indicate that having a larger baseline by including widely separated detectors helps for sky position accuracy, and that the involvement of a fourth, km-scaled, detector besides the two LIGO facilities and Virgo is highly desirable.

3.2. Fundamental Physics

The measurements of GWs emitted by the coalescence of compact binary systems enables an empirical access to the strong field, non-linear dynamics of the fundamental gravity theory. The result of matched-filtering, used in the search for signals from coalescing binaries, is particularly sensitive to the time-varying phase of the oscillating GW signal. During the inspiral phase, when the binary constituents are widely separated, the GW phase Ψ admits an analytical representation which in the frequency

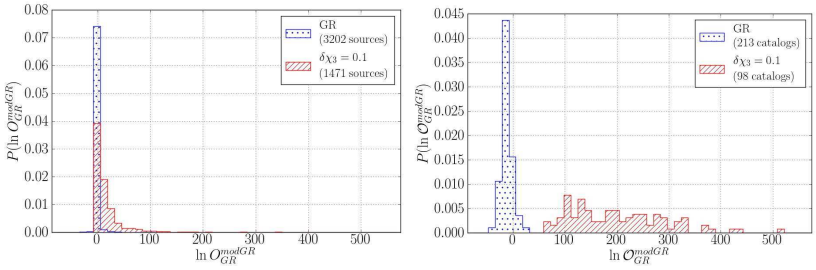

Figure 8. Distribution of Bayes factor for competing hypotheses (GR vs. non-GR) for GR and non-GR signals obtained by varying ψ_3. (a) refers to odds ratio for single signals, (b) to catalogs made of 15 signals, from Li et al. (2012b).

domain reads

$$\Psi(t_c, \phi_c, M_c, \eta; f) = 2\pi f t_c - \phi_c - \pi/4 + \sum_{i\geq 0} \left[\psi_i + \psi_i^{(l)} \ln f\right] (\pi M_c f)^{(i-5)/3} . \qquad (5)$$

In the case of GR the coefficients $\psi_i, \psi_i^{(l)}$ are known up to some perturbative order in terms of the physical properties of the binary constituents (mass ratio η and spins). However within a Bayesian framework one can compare the validity of the GR hypothesis (all the ψ_i coefficients as predicted by GR) with alternative ones allowing (some of) the ψ_is to take non-GR values. In particular, Bayesian inference allows the computation of Bayes' factors B_{H_i} between competing hypotheses $H_{i,j}$ (as well as the marginalised posterior density functions on the unknown signal parameters). After computing a background for detection statistics by evaluating the Bayesian odds ratio $O^{H_i}_{H_j} \equiv B_{H_i}/B_{H_j}$ between competing hypotheses, it is possible to assess if data containing GW signals favour the hypothesis supporting GR or a violation of it. The analysis performed in Li et al. (2012b,a) showed that with a single detection of a binary neutron star inspiral at moderate signal-to-noise ratio SNR ($8 < \mathrm{SNR} < 45$) it is not possible to distinguish the fundamental theory ruling the binary inspiral, as the distribution of Bayes factor ratio overlap for GR and non-GR injection. However it also showed that *repeated* detections can indicate a deviation from GR, as fig.8 shows in the case study of a signal with a 10% variation in ψ_3 with respect to its GR value. Note that with present observations/experiments not even ψ_1 is tested at the $O(1)$ level.

Another interesting application of GWs to GR testing is investigated in Kamaretsos et al. (2012), where it is suggested that comparing signals from the last stage of a coalescence, the ring-down, it is possible to check for consistency of the signal with GR and even extract physical information on the binary constituents (even though the SNRs that should be collected by the advanced detectors may be too small for this purpose).

Finally, the interior of neutron stars, which is likely made of un-confined nuclear matter, may provide an insight into nuclear physics, as the normal mode oscillations of neutron stars are the only probe of their internal structure, see Tsui & Leung (2005).

3.3. Cosmology

A direct detection of a stochastic background of GWs of cosmological origin is another possible goal of the GW search, even though there are no compelling candidates. A

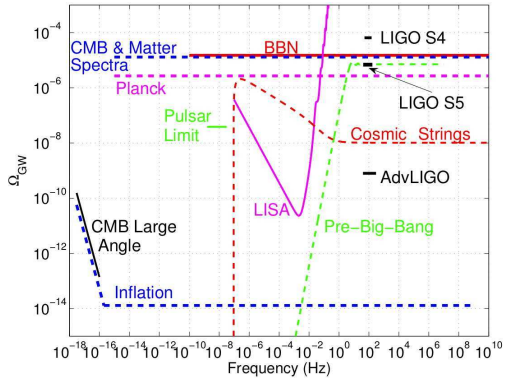

Figure 9. The landscape for GW detection of cosmological origin, from Abbott et al. (2009).

non-trivial upper limit has been set in Abbott et al. (2009), where in the band-width of highest sensitivity of the two LIGO detectors, the amount of stochastic GWs has been constrained to a quantity smaller than the *nucleosynthesis bound*. The possibility that a correlation of two advanced LIGO detectors at design sensitivity may detect a background originating from the cosmological evolution or by a cosmic string network, as shown in fig.9, has to be considered highly speculative.

An outstanding application of GWs to cosmology is represented by the use of signals from inspiral binaries as standard sirens, as first pointed out by Schutz (1986). For sources at cosmological distance, the observer time t_o is related to the source time t_s by $dt_o = (1+z)dt_s$ and analogously for the frequency f. The inspiral signal $h(t)$ from a binary system at coordinate (luminosity) distance $D(D_L)$ and red-shift $z = a(t_o)/a(t_s) - 1$ can be written as

$$h(t_o) = \frac{G_N(f_s(1+z))^{2/3}M_c^{5/3}}{a(t_o)D}\cos(\phi(t_s/M_c,\eta)) = \frac{f_o^{2/3}\,(M_c(1+z))^{5/3}}{D_L}\cos(\phi(t_o(t_s)/M_c,\eta))\,. \tag{6}$$

It is not possible to extract the red-shift value from the GW shape, as it is completely degenerate with M_c and it can be absorbed in the definition of the quantity $\mathcal{M}_c \equiv (1+z)M_c$. However coalescing binaries offer a well calibrated signal, since $f_o, \mathcal{M}_c$ can be obtained from the time behaviour of the phase and then its amplitude can be used to determine the luminosity distance. Once combined with an independent, electromagnetic determination of the red-shift it can lead to a measure of the Hubble law $z = H_0 D_L$, which defines the Hubble constant H_0. Moreover, as shown with an example by DelPozzo (2011), even in absence of an electromagnetic counterpart, the value of the Hubble constant can be obtained by GW triggers only, provided a *complete* catalog of galaxies is available. With repeated detection of GWs and by considering all the galaxy hosts consistent with the sky position and distance posterior distributions recovered from the GW signals, fig.10 shows that with a detection of $O(50)$ GW events at moderate SNR (< 35) and at red-shifts $z \lesssim 0.1$, the value of H_0 can be constrained to few percent.

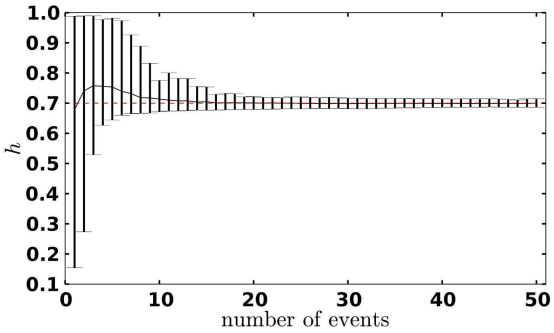

Figure 10. Confidence interval for the reduced Hubble constant h defined as $h \equiv H_0/100\,\mathrm{km/s/Mpc}$ as a function of the number of events considered, with error bars corresponding to 95% confidence interval. From DelPozzo (2011).

References

Abadie, J., et al. (LIGO Scientific and Virgo Collaborations) a. arXiv:1201.5999[gr-qc]
— b. arXiv:1112.6005[astro-ph.CO]
Abadie, J., et al. (The LIGO Scientific and Virgo Collaborations) 2010, Class. Quant. Grav., 27. arXiv:1003.2480[astro-ph.HE]
Abadie, J., et al. 2011a, Astrophys. J., 7372. arXiv:1104.2712[astro-ph.HE]
Abadie, J., et al. (The LIGO Scientific and Virgo Collaborations) 2011b, Astrophys. J., 734, L35. arXiv:1011.4079[astro-ph.HE]
Abadie, J., et al. (LIGO Scientific Collaboration and Virgo) 2011c
Abadie, J., et al. (The LIGO Scientific and Virgo Collaborations) 2012a. arXiv:1202.2788[gr-qc]
— 2012b, Phys. Rev. D, 85. arXiv:1111.7314[astro-ph.HE]
Abbott, B. P., et al. (LIGO Scientific and Virgo Collaborations) 2009, Nature, 460. arXiv:0910.5772[astro-ph.CO]
— 2010, Astrophys. J., 713. arXiv:0909.3583[astro-ph.HE]
Adrian-Martinez, S., et al. (The LIGO Scientific and Virgo Collaborations) 2012. arXiv:1205.3018[astro-ph.HE]
Ando, S., Beacom, J. F., & Yuksel, H. 2005, Phys. Rev. Lett., 95. arXiv:astro-ph/0503321
Briggs, M. S., et al. (The LIGO Scientific and Virgo Collaborations) 2012. arXiv:1205.2216[astro-ph.HE]
DelPozzo, W. 2011. arXiv:1108.1317[astro-ph.CO]
Evans, P. A., et al. (LIGO Scientific and Swift Collaborations) 2012. arXiv:1205.1124[astro-ph.HE]
Kamaretsos, I., Hannam, M., & Sathyaprakash, B. S. 2012. arXiv:1207.0399[gr-qc]
Klimenko, S., et al. 2011, Phys. Rev. D, 83. arXiv:1101.5408[astro-ph.IM]
Li, T. G. F., et al. 2012a, Phys. Rev. D, 85. arXiv:1110.0530[gr-qc]
— 2012b, J. Phys. Conf. Ser., 363. arXiv:1111.5274[gr-qc]
Maggiore, M. 2008, Gravitational Waves. Vol. I: Theory and Experiments (Oxford University Press)
Piro, L. 2005, Nat, 437
Schutz, B. F. 1986, Nat, 323
Tsui, L. K., & Leung, P. T. 2005, Phys. Rev. Lett., 95. arXiv:astro-ph/0506681
Veitch, J., et al. 2012, Phys. Rev. D, 85. arXiv:1201.1195[astro-ph.HE]
Weisberg, J. M., & Taylor, J. H. 1984, Phys. Rev. Lett., 52